Measurements of Photon Correlations in Partially Coherent Light*

D. B. SCARL
Department of Physics, Polytechnic Institute of Brooklyn, Brooklyn, New York 11201
(Received 10 May 1968)

Measurements have been made of the distribution in time of arrival of photons produced in a low-pressure Hg^{198} discharge. Sufficient calibration was done so that the measurements could be directly compared with the predictions of a calculation of $G^{(2)}(x_1,x_2,x_2,x_1)$, the second-order coherence function. Correlations were observed in a mixture of light from two independent sources and between orthogonally polarized components of a beam initially in a pure polarization state.

INTRODUCTION

WE have performed two sets of measurements of photon time-of-arrival distributions in beams of Gaussian light. The first set of measurements was designed to investigate the second-order interference between independently generated photons from widely separated parts of a light source; essentially photons from two separate sources. The second set of measurements was of the second-order interference of photons in orthogonally polarized beams of light. In this case, first-order interference is impossible, but second-order interference is easily observed. In each case the interference consists of a 1-nsec peak 11% above the background in the curve of counting rate versus time delay for two consecutive photons.

In both these experiments light from a single very narrow spectral line produced in a low-pressure mercury discharge was collimated to a high degree of spatial coherence and was allowed to fall on the cathodes of two photomultipliers. When an output pulse from one photomultiplier indicated the arrival of a photon, the time interval until the arrival of the next photon at the other tube was recorded. This distribution in time intervals shows an excess number of counts for time intervals short compared with the coherence time of the light, the well-known "bunching" of photons. This second-order interference effect was used to investigate correlations between photons from two sources and between orthogonally polarized photons.

Photon time-of-arrival measurements are an extension of the pioneering experiments of Hanbury Brown and Twiss, who first extended second-order interference measurements from the rf [1] region to the optical region of the electromagnetic spectrum. These first measurements were done by multiplying together the outputs of two square-law detectors in partially coherent fields produced by laboratory sources[2] and stars.[3] Rebka and Pound,[4] and subsequently three other groups,[5] later observed the same second-order interference by doing photon coincidence counting experiments on laboratory-produced light. Recently[6] the photon coincidence experiment has been modified so that a distribution in delay times can be measured in one run. These photon time-of-arrival experiments show a reasonably large and easily detectable second-order interference effect.

APPARATUS

The light source was a 7-mm-diam 100-mm-long quartz tube filled with argon to a pressure of 2 Torr and containing about 1 mg of Hg^{198}. An electrodeless discharge was maintained in the tube by placing it in an untuned coaxial cavity excited by about 10 W of 3-Gc/sec rf power. Light was taken from one side of the discharge tube, the opposite side being cooled by an air stream strong enough to keep the outside of the tube near room temperature. Cooling only the back side of the tube helped to prevent forcing the light to leave the hot central gas through a layer of cooler gas, a situation which encourages line reversal.

The light from the discharge tube escaped from the microwave cavity through a $\frac{1}{4}$-in. hole and illuminated

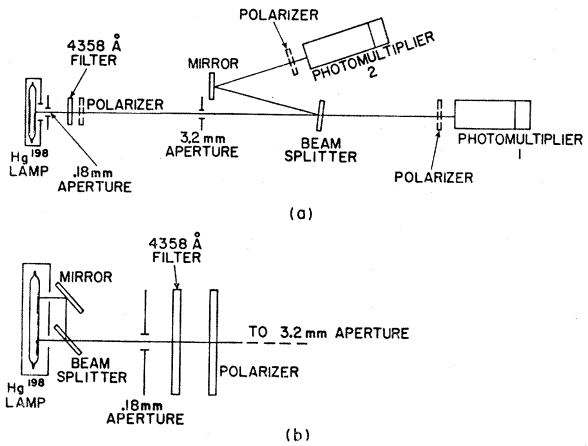

FIG. 1. The experimental arrangement for (a) the single-source and polarization runs and (b) the double-source run. The drawings are not to scale.

* Supported in part by the Science Development Program of the National Science Foundation, Grant No. SDP-GU-1557.

[1] R. Hanbury Brown, R. C. Jennison, and M. D. Das Gupta, Nature **170**, 1061 (1952).

[2] R. Hanbury Brown and R. Q. Twiss, Nature **177**, 27 (1956); Proc. Roy. Soc. (London) **A242**, 300 (1957); **A243**, 291 (1957).

[3] R. Hanbury Brown and R. Q. Twiss, Nature **178**, 1046 (1956).

[4] G. A. Rebka and R. V. Pound, Nature **180**, 1035 (1957).

[5] E. Brannen, H. T. Ferguson, and W. Wehlau, Can. J. Phys. **38**, 871 (1958); R. Q. Twiss and A. G. Little, Australian J. Phys. **12**, 77 (1959); B. L. Morgan and L. Mandel, Phys. Rev. Letters **16**, 1012 (1966).

[6] D. T. Phillips, H. Kleiman, and S. P. Davis, Phys. Rev. **153**, 113 (1967); D. B. Scarl, Phys. Rev. Letters **17**, 663 (1966).

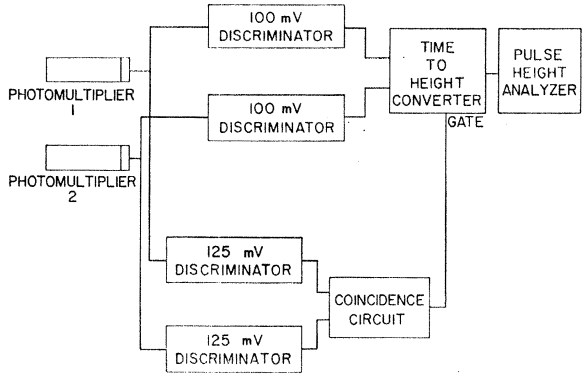

FIG. 2. The electronic double discriminator and time-to-height conversion system.

a 0.18-mm-diam aperture about 1 in. away (Fig. 1). A band-pass interference filter with a central wavelength of 4360 Å and a 70-Å bandwidth assured that only the light from the 4358-Å mercury line was used. In some cases a Polaroid right-hand circular polarizer was placed immediately after the interference filter.

A second aperture 135 cm from the first and 3.19 mm in diameter provided a slowly diverging beam that was 60% spatially coherent. After passing through the second aperture the light struck a TiO_2-coated glass beam splitter at an angle of 7°. Use of the beam splitter at almost normal incidence made the reflection (55%) and transmission (45%) coefficients independent of polarization to within about 1%. The transmitted light illuminated a spot about $\frac{1}{8}$ in. in diameter in the center of the cathode of photomultiplier 1. The reflected light was redirected by a first-surface aluminized mirror and illuminated a $\frac{1}{8}$-in. spot at the cathode of photomultiplier 2. The optical path from the splitter to each photomultiplier was 14.0 in. When used, a piece of Polaroid HN38 linear polarizer was placed 4 in. in front of each photocathode.

The photomultipliers were RCA 8575's run at 3000 V between anode and cathode. They were covered with a copper foil at cathode potential (−3000 V), two layers of Mylar, a Mumetal shield, and an aluminum light-tight housing. The anode pulses from each tube were divided by a 50-Ω matched tee and led to two Chronetics model 110 discriminators (Fig. 2). One discriminator accepted all pulses above 100 mV and produced standardized 250-mV-high 30-nsec-long output pulses. These pulses were overlapped with similar pulses from a discriminator connected to the other photomultiplier in a time-to-height converter which converted the pulse overlap time to a pulse height. The pulses from tube 2 were delayed by 15 nsec with respect to the pulses from tube 1 so that simultaneous photoelectrons produced an output pulse in the middle of the time-to-height converter's range. The output pulses from the time-to-height converter were analyzed and stored in the first 200 channels of a TMC 400C pulse-height analyzer.

The second discriminator connected to photomultiplier 1 was set to accept only pulses over 125 mV and its 15-nsec-long output pulses were sent to a coincidence circuit. The second input to this circuit came from the output of a 125-mV discriminator connected to tube 2. The time-to-pulse-height converter was gated on only when there was an output pulse from the coincidence circuit indicating that there had been photomultiplier output pulses over 125 mV from each tube and that the two pulses were within 30 nsec of each other. For pulses very near threshold the 100-mV discriminator output pulses appear with a time delay that is inversely proportional to the input pulse height. The double discriminator system was used to eliminate this time slewing by allowing only pulses well above the threshold of the timing discriminator to be analyzed.

The coincidence counting rate varied between 4 and 0.3 counts per second depending on the number of polarizers in the beam. The memory of the pulse-height analyzer was read out onto paper tape once each day but not reset to zero. At the end of a run (2 to 20 days) the data on the final tape were plotted. No adjustments of any kind were made to the data.

CALIBRATION

Mercury Lamp

The power spectrum of the 4358-Å Hg^{198} line was measured using a Fabry-Perot interferometer which had a $\frac{3}{4}$-in. clear aperture and a measured finesse of 12. The interferometer was piezoelectrically scanned and aligned. The mirrors were flat to $\frac{1}{20}$ of a wavelength of sodium light and aluminized to a reflectivity of 80%. The mirrors were separated by $\frac{1}{2}$ in. for one series of runs and by $2\frac{1}{4}$ in. for a second series.

A real image of the ring pattern was formed by a 50-cm focal length lens which focused the center of the pattern onto a 0.2-mm aperture in front of a 931 A photomultiplier. The output of the photomultiplier, corresponding to the intensity of the central bright spot of the interference pattern, was amplified and plotted by a chart recorder. For each run the length of the cavity was scanned over a range of about five half-wavelengths by a sawtooth voltage applied to the piezoelectric cylinder on which one mirror was mounted. The width of the peaks on the chart records was corrected for the interferometer finesse and divided by the peak-to-peak distances to provide the full width at half-maximum of the Hg^{198} line in terms of the distance between the interferometer mirrors. The spectral width was found to vary with the excitation of the lamp and ranged from 1.6±0.3 to 2.0±0.3 Gc/sec (FWHM) under the conditions used for the various correlation runs. Expressed in terms of wavelength, these widths are 0.010±0.002 Å and 0.013±0.002 Å. The line shape as a function of angular frequency ω can be expressed as a Gaussian with standard deviations σ_ω of 4.3×10^9 and 5.3×10^9 rad/sec in the two cases.

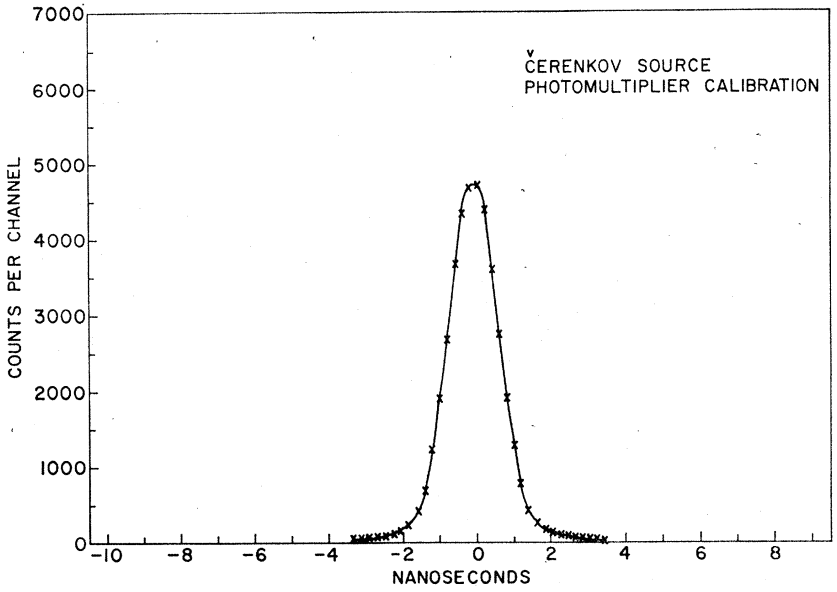

FIG. 3. The time spectrum of output pulses from the two 8575 photomultipliers with coincident single-photon inputs. The full width of the curve at half-maximum is 1.5 nsec. The curve is drawn by hand to fit the points.

Electronics

The fast electronics and pulse-height analyzer were calibrated in nsec per channel by using a fast-rise pulse generator to send simultaneous pulses to the inputs of the four discriminators. The pulse-height analyzer channel in which these counts were stored corresponds to zero time delay. Introducing a 77.25-in. length of RG58A/U cable, in which the velocity of propagation is 65.9% of the velocity of light, before one discriminator delayed its input pulse by 10.0 nsec. The pulse-height analyzer gain was adjusted to throw the resulting counts into the 50th channel above the zero-time channel. With the 10-nsec delay cable inserted before the other discriminator, the counts fell 50 channels below the zero-time channel. In this way the electronics were calibrated to 200 psec per channel with respect to a known length of coaxial cable. Running with a pulser input, all of the recorded pulses fell into a single channel and the position of this channel was stable over periods of days. This indicates a time resolution and stability of the electronics of better than 200 psec.

Photomultiplier Time Resolution

The spread in time of photomultiplier output pulses for coincident input photons was measured by shining a weak source of simultaneous single photons on the two photocathodes. The sumultaneous photon source was made by allowing a collimated beam of electrons from a 100-μCi $Sr^{90}Y^{90}$ source to produce Čerenkov light in Plexiglas. The electrons have a maximum energy of 2.2 MeV and a maximum range of about $\frac{1}{2}$ in. Each electron produces at most 50 photons in the wavelength interval between 3000 and 7000 Å. These photons leave the Plexiglas simultaneously. With the photocathodes about 5 in. away from the Čerenkov source most of the photons produced by each electron go undetected, but two photons produced by one electron do hit the two cathodes often enough to give a coincidence counting rate of about one event per second. After a running time of several hours the pulse-height analyzer time distribution looks like Fig. 3. This curve of photomultiplier time resolution is a Gaussian with full width at half-maximum of 1.5 nsec, corresponding to a standard deviation of 0.63 nsec.

Photon Detection Efficiency and Noise

The light energy at each photocathode due to the Hg source was measured by replacing each photomultiplier by a 6655a phototube that had been calibrated against a blackbody source. With no polarizers in the beam, 260 000 photons/sec arrived at each photocathode. When viewing the same beam, the 8575 photomultipliers produced 31 000 output pulses per second which were above the 125 mV required to trigger the output discriminators, leading to a photon detection efficiency of 12%. Since the cathode efficiency is near 25% on these tubes, this indicated that 50% of the single electrons leaving the cathode produced output pulses higher than 125 mV. The photon detection efficiency does not affect the time-of-arrival distributions since only the ratio of peak height to background height is wanted, and the photodetection efficiency affects peak and background equally.

At 24-h intervals during each correlation run an electromagnetic shutter was closed, interrupting the Hg lamp beam. The noise rates from each photomultiplier varied from 200 to 600 counts/sec, depending on the temperature and humidity. This low noise rate (400 to 1200 electrons/sec leaving the 16.5-cm^2 cathode) was only achieved after the tubes had been in the dark for several days.

COUNTING-RATE CALCULATION

Second-Order Correlation Function

Prediction of the distribution of photon arrival time differences and calculation of the associated second-order coherence function has been done both semiclassically[2,7] and quantum-mechanically.[8,9] The most instructive way to calculate the counting rate for the annihilation of two photons separated in time by Δt is to use the elegant formulation of quantum coherence theory developed by Glauber.[8] The counting rate of a 100% efficient detector when the field is initially in a pure state $|i\rangle$ is

$$R_{\text{ideal}}=\sum_f |\langle f|A_1(t)A_2(t+\Delta t)|i\rangle|^2, \quad (1)$$

where $\langle f|$ is a suitable but unmeasured final state, and A_1 and A_2 are field operators which are the positive-frequency parts of the electric field at the two photocathodes. It should be pointed out that the distribution in delay times measured with a time-to-height converter corresponds to the probability of detecting a photon at time t and another at time $t+\Delta t$ only when there is no other photon detected between t and $t+\Delta t$, since the converter records the time difference between a detected photon and the *next* detected photon. For the present experiment, the average interval between events is so long compared with the time interval of interest that the measured distribution is indistinguishable from the actual distribution in arrival times. The general case of two-photon measurements with a time-to-height converter is treated in Ref. 10.

When the sum is performed in Eq. (1), the counting rate becomes the expectation value in the state $|i\rangle$ of a product of four field operators

$$R_{\text{ideal}}=\langle A_2^\dagger A_1^\dagger A_1 A_2\rangle_i. \quad (2)$$

For fields produced by thermal light sources the initial state of the field is not a pure state but a mixed state made up of a sum of pure states with statistically varying amplitudes and phases. This mixture is described by ρ, the density matrix for the field, in terms of which the expectation value of the product of field operators becomes

$$R_{\text{ideal}}=\text{Tr}(\rho A_2^\dagger A_1^\dagger A_1 A_2). \quad (3)$$

A comparison between this expression for the two-photon counting rate and the second-order correlation function as usually defined in the theory of partial coherence shows that they are identical. In general, the nth-order correlation function is defined as

$$G^{(n)}(x_1,x_2,\cdots,x_n;x_{n+1},\cdots,x_{2n}) = \text{Tr}[\rho A^\dagger(x_1)A^\dagger(x_2)\cdots A^\dagger(x_n)A(x_{n+1})\cdots A(x_{2n})], \quad (4)$$

where x_i denotes the space-time point $(t_i,\mathbf{r}_i)$. In particular, the first-order correlation function that arises in most of the usual interference experiments is

$$G^{(1)}(x_1,x_2)=\text{Tr}(\rho A^\dagger(x_1)A(x_2)), \quad (5)$$

expressing the correlation between the field evaluated at two different space-time points. The second-order function is

$$G^{(2)}(x_1,x_2,x_3,x_4)=\text{Tr}(\rho A^\dagger(x_1)A^\dagger(x_2)A(x_3)A(x_4)). \quad (6)$$

The special case of $G^{(2)}$ that corresponds to the two-photon time distribution function is that in which $x_3=x_2$ and $x_4=x_1$, that is, only two space-time points are involved:

$$G^{(2)}(x_1x_2x_2x_1)=\text{Tr}(\rho A_1^\dagger A_2^\dagger A_2 A_1)=R_{\text{ideal}}, \quad (7)$$

and it can be seen that a measurement of the two-photon counting rate corresponds to a measurement of the second-order correlation function at two space-time points. The dependence of $G^{(2)}$ on the spatial difference between the points x_1 and x_2 is integrated to provide the spatial coherence factor. The two-photon counting rate data are presented as the dependence of $G^{(2)}$ on Δt, the time difference between the points x_1 and x_2.

For thermal light, with its characteristic Gaussian distribution of amplitudes, it is possible to show that[8]

$$G^{(2)}(x_1x_2x_2x_1)=G^{(1)}(x_1x_1)G^{(1)}(x_2x_2) + G^{(1)}(x_1x_2)G^{(1)}(x_2x_1). \quad (8)$$

This reduction of the second-order correlation function to a sum of products of first-order correlation functions results from the vanishing of terms with an unmatched number of photon creation and annihilation operators when the exponential (Gaussian) amplitude integrals and the four sums over propagation vectors are done.

The first-order correlation functions for a polarized quasimonochromatic cross spectrally pure Gaussian light source are

$$G^{(1)}(x_1x_1)=G^{(1)}(x_2x_2)=I, \quad (9a)$$

$$G^{(1)}(x_1x_2)=[G^{(1)}(x_2x_1)]^*=Iq(\Delta\mathbf{r})f(\Delta t), \quad (9b)$$

where

$$q(\Delta\mathbf{r})=\int p(\mathbf{k})e^{i\mathbf{k}\cdot\Delta\mathbf{r}}d\mathbf{k}, \quad (10a)$$

$$f(\Delta t)=\int g(\omega)e^{i\omega t}d\omega. \quad (10b)$$

I is the total light intensity, $p(\mathbf{k})$ is its angular distribution, and $g(\omega)$ is its frequency distribution. For a plane-wave beam completely spatially coherent, $p(\mathbf{k})$

[7] L. Mandel and E. Wolf, Rev. Mod. Phys. **37**, 231 (1965).
[8] R. J. Glauber, Phys. Rev. **131**, 2766 (1963); in *Quantum Optics and Electronics*, edited by C. DeWitt, A. Blandin, and C. Cohen-Tannoudji (Gordon and Breach, Science Publishers, Inc., New York, 1965).
[9] John R. Klauder and E. C. G. Sudarshan, *Fundamentals of Quantum Optics* (W. A. Benjamin, Inc., New York, 1968).
[10] F. Davidson and L. Mandel, J. Appl. Phys. **39**, 62 (1968).

$=\delta(\mathbf{k}-\mathbf{k}_0)$, $q(\Delta\mathbf{r})=\exp i\mathbf{k}_0\cdot\Delta\mathbf{r}$, and the second-order correlation function becomes

$$G^{(2)}(x_1x_2x_2x_1)=I^2(1+|f(\Delta t)|^2). \quad (11)$$

For the 4358-Å Hg line used in the present work, the Doppler-broadened line shape is a Gaussian function of frequency centered at ω_0 and with standard deviation σ_ω,

$$g(\omega)=(2\pi\sigma_\omega)^{-1/2}e^{-(\omega-\omega_0)^2/2\sigma_\omega^2}. \quad (12)$$

Its Fourier transform,

$$f(\Delta t)=e^{i\omega_0\Delta t}e^{-(\Delta t)^2/2\sigma_t^2}, \quad (13)$$

is a Gaussian function of time with standard deviation $\sigma_t=1/\sigma_\omega$. Finally, the two-photon counting rate for a pair of noiseless, 100%-efficient detectors as a function of the difference in time of detection of the two photons, for a completely spatially coherent beam in a pure polarization state, would be

$$G^{(1)}(x_1x_2x_2x_1)=I^2(1+e^{-(\Delta t)^2/2\sigma_T^2}), \quad (14)$$

where $\sigma_T=\sigma_t/\sqrt{2}$.

Expected Counting Rate

For light from a single Hg line of width 1.6 Gc/sec the standard deviation of the square of the Fourier transform of the line shape is 0.17 nsec. With this value of σ_T, Eq. (11) for the counting rate as a function of difference in arrival time for a photon pair predicts a background rate of I^2 independent of Δt and a peak centered at zero time delay of height I^2 above the background and 0.17 nsec wide. To convert Eq. (14) into an expression that corresponds to the actual experimental conditions it must be modified to take into account one effect that decreases the entire counting rate, three effects that lower the relative peak height, and one effect that tends to both lower the relative peak height and increase its width. The 12% detection efficiency of the photomultipliers decreases the entire counting rate, leaving the peak-to-background ratio unchanged. The effects which lower the relative peak height are the lack of complete spatial coherence in the beam, the polarization state of the beam, and the spurious counts due to photomultiplier noise. To take these into account a correlation factor C, which is the product of factors S due to the incomplete spatial coherence, N due to photomultiplier noise, and P due to the polarization state of the beam, is allowed to multiply the exponential term in the expression for the counting rate.

The finite time-resolution capabilities of the photomultipliers increase the width of the peak and lower its height, keeping the number of counts under the peak constant. The function $|f(\Delta t)|^2$ must be convoluted with the photomultiplier time resolution function to give the expected experimental curve. Since both functions are Gaussian, this has the effect of widening the peak by a factor of σ_p/σ_T and reducing its height by σ_T/σ_p. The width σ_p is the square root of the sum of the squares of the photomultiplier time resolution and σ_T.

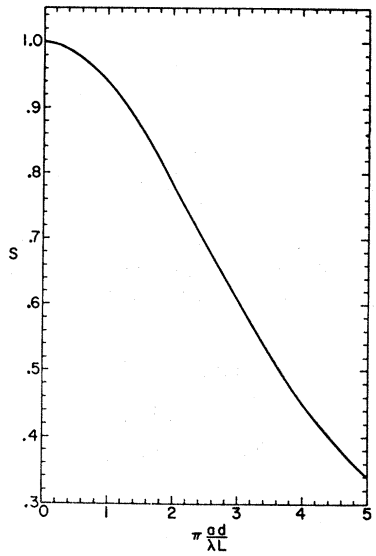

FIG. 4. A plot of the spatial coherence factor S versus $\pi da/\lambda L$ for light of wavelength λ passing through two circular apertures of diameter a and d, separated by a distance L. For the conditions of this experiment, $\pi ad/\lambda L$ was 3.04 and S was 0.60.

With these modifications the two-photon counting rate for a real detector becomes

$$R(\Delta t)=R_0\left(1+C\frac{\sigma_T}{\sigma_p}e^{-(\Delta t)^2/2\sigma_p^2}\right), \quad (15)$$

where R_0 contains the light intensity and the photomultiplier detection efficiencies and noise rates. For the experiments recorded here the correlation factor C was between zero and 0.57, σ_p was 0.66 nsec, and σ_T/σ_p was between 0.21 and 0.26. Under the conditions of these experiments the width of the peak is largely influenced by the photomultiplier time resolution and its height is directly proportional to the coherence of the beam.

Spatial Coherence Factor

The spatial coherence of the beam is determined by the size and separation of the 0.18- and 3.2-mm apertures. If the departure of the beam from a uniform plane wave is taken into account, $|q(\Delta\mathbf{r})|^2$ must be integrated over the second aperture to provide the spatial coherence factor S.

For a uniformly illuminated circular first aperture of diameter a, $q(\Delta\mathbf{r})$ evaluated in the plane of the second aperture becomes

$$q(\Delta r)=2\pi(\tfrac{1}{2}a)^2\left[J_1\left(\frac{2\pi}{\lambda L}\frac{a}{2}\Delta r\right)\right]\Big/\left(\frac{2\pi}{\lambda L}\frac{a}{2}\Delta r\right), \quad (16)$$

where λ is the wavelength of the light, L is the distance between apertures, and J_1 is the usual Bessel function.

The integral of $|q(\Delta r)|^2$ over all pairs of points within the second aperture is

$$S(\pi ad/\lambda L)=\int_0^{2\pi}\int_0^{2\pi}\int_0^{d/2}\int_0^{d/2}\left[\frac{J_1((\pi a/\lambda L)[r_1^2+r_2^2-2r_1r_2\cos(\theta_1-\theta_2)]^{1/2})}{(\pi a/\lambda L)[r_1^2+r_2^2-2r_1r_2\cos(\theta_1-\theta_2)]^{1/2}}\right]^2\times r_1dr_1d\theta_1r_2dr_2d\theta_2, \quad (17)$$

where d is the diameter of the second aperture. This expression for the spatial coherence was numerically integrated and the results are shown as a function of $ad/\lambda L$ in Fig. 4. For the aperture sizes and separation in the present experiments, $S=0.60$.

Photomultiplier Noise

Since the pulse-height distribution of photomultiplier output pulses caused by single electrons leaving the cathode is roughly exponential and has almost the same shape for photoelectrons and for noise electrons, it is impossible to completely separate photoelectron counts from noise counts. The noise counts are completely uncorrelated and reduce the correlation factor. If S_1 and S_2 are the photoelectron counting rates for tubes 1 and 2, and N_1 and N_2 are the noise rates, the contribution of the noise counts to the correlation factor is

$$N=S_1S_2/(S_1+N_1)(S_2+N_2). \quad (18)$$

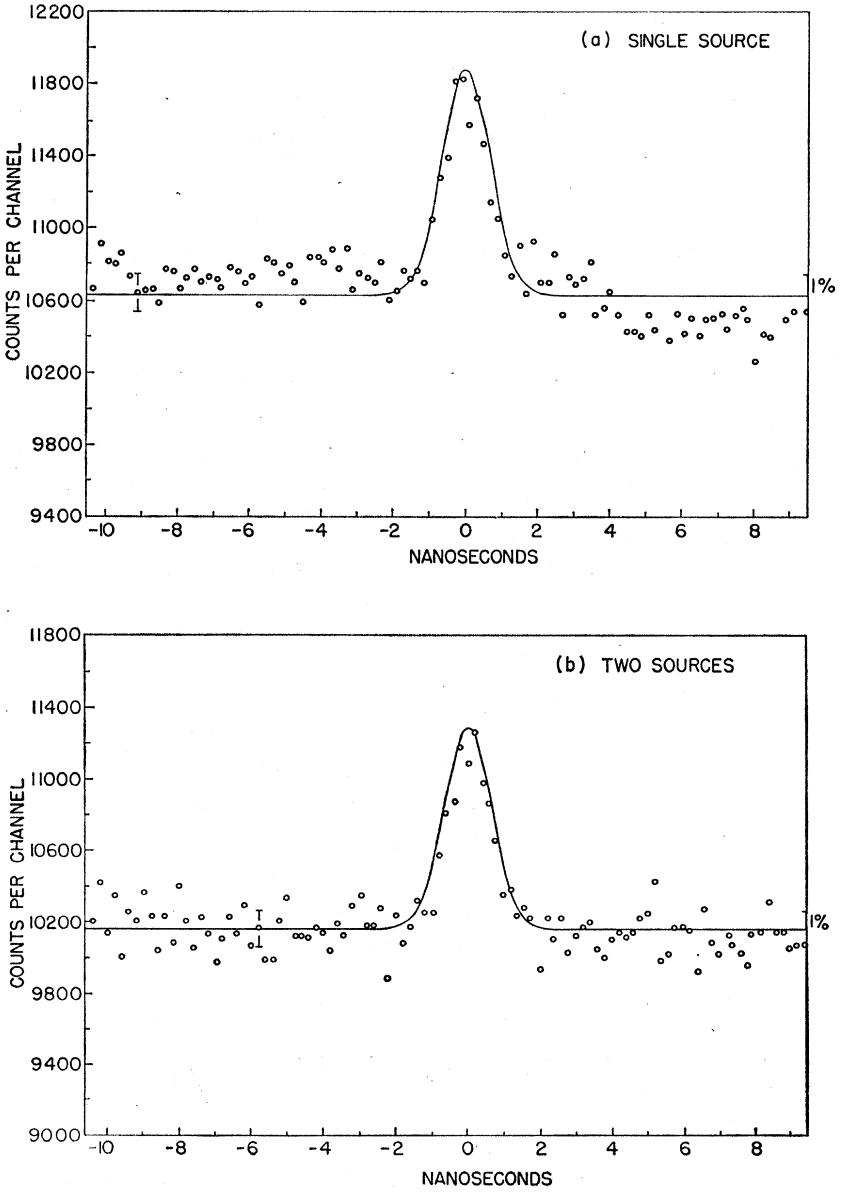

FIG. 5. The two-photon time distribution $R(\Delta t)$ versus Δt for photons from (a) a single area of the mercury discharge tube and (b) two areas of the tube separated by 1.5 in. The solid lines are the curves predicted on the basis of the coherence of the light and the resolution of the photomultipliers. All the experimental points have the same purely statistical error bars.

N_1 and N_2 were each about 300 counts/sec. S_1 and S_2 ranged from 3000 to 30 000 counts/sec due to the 30% absorption of each of the polarizers in the beam. N was between 0.78 and 0.98 for the various runs.

RESULTS

Single Source

The counting rate as a function of time delay for light from the 4358-Å Hg line is shown in Fig. 5(a). Horizontal polarizers which transmitted the horizontal polarization component of the light and absorbed the vertical component were placed in front of each phototube. For this completely polarized light, the polarization coherence factor P is equal to 1. For this run N was 0.94, C was 0.57, and σ_T was 0.13 nsec. Events were accumulated over a total period of 170 h. The expected counting rate which is plotted as a solid curve in Fig. 5(a) was

$$R(\Delta t)=R_0(1+0.12e^{-(\Delta t)^2/2(0.65)^2}). \quad (19)$$

The measured points agree well with this curve.

Double Source

Beams from two regions of the Hg discharge tube separated by 1.5 in. in a direction perpendicular to the viewing direction were combined using a TiO_2 beam splitter and illuminated the first aperture as in Fig. 1. The remainder of the apparatus was identical to that used to make the above measurement of correlations

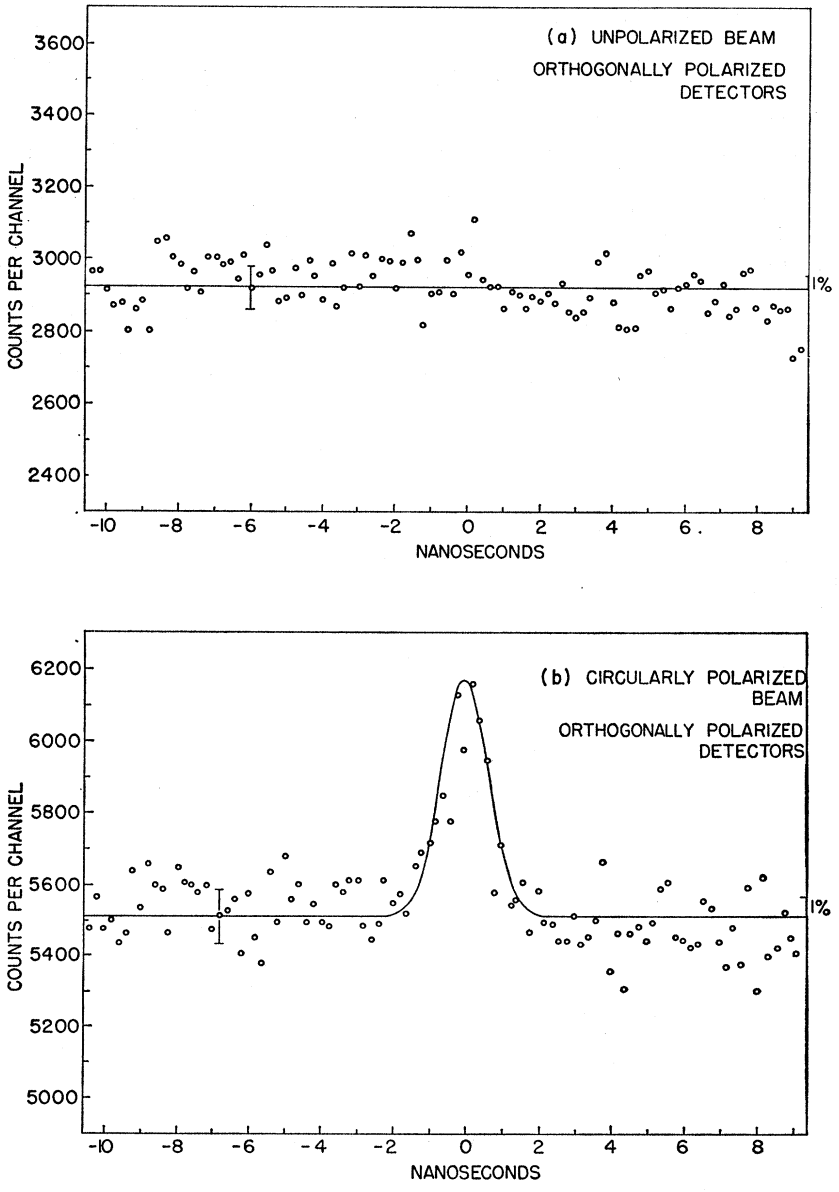

FIG. 6. The two-photon time distribution $R(\Delta t)$ versus Δt for (a) detectors sampling orthogonally polarized states derived from an originally unpolarized field and (b) detectors sampling orthogonally polarized states derived from an originally polarized field. The solid lines are the predicted curves; all points have the same statistical error bars.

from a single region of the discharge tube. The correlation factor and the predicted curve of $R(\Delta t)$ were also essentially identical to the single source measurement. Events were accumulated for 160 h. The resulting photon correlation data are shown in Fig. 5(b), and are seen to be identical to the single source data. This result indicates that correlations between photons from two independent sources can be seen if the photons are made indistinguishable by arranging that their central frequencies and propagation vectors overlap. This would seem to confirm that photon correlations do not arise from stimulated emission or other atomic cooperation effects in the source, but from the indistinguishability of the photons themselves. If photons from source A were correlated only with other photons from source A and not with photons from source B, the height of the peak in the measurement of $R(\Delta t)$ would be half the observed height.

Orthogonal Polarization

In this run, light from a single source illuminated the first aperture. A horizontal polarizer was placed in front of one photomultiplier and a vertical polarizer was placed in front of the other. The signal-to-noise contribution to the correlation factor was $N=0.88$ and σ_T was 0.17 nsec. Since two orthogonally polarized components of a light beam originally in a mixed state of polarization (unpolarized) are statistically independent, the polarization contribution to the correlation factor is zero and the counting rate is expected to be independent of Δt.[7] Figure 6(a) shows the data for orthogonal polarizers in an unpolarized beam for a counting period of 40 h. No correlation peak is evident.

Orthogonal Polarization in a Polarized Beam

The apparatus in this run was identical to that in the previous run except that a right-hand circular polarizer which absorbed the horizontally polarized component of the original beam and converted the vertical component to right-hand circular polarization was placed immediately after the first aperture. The beam leaving this polarizer was in a pure polarization state: an eigenstate of circular polarization but not an eigenstate of linear polarization. For a pure polarization state the horizontal and vertical components are completely correlated and the polarization part of the correlation factor in the expression for $R(\Delta t)$ is unity. The correlation factor was 0.46, leading to a curve of $R(\Delta t)$ with an expected peak height of 12%, the solid curve in Fig. 6(b). The measured distribution of difference in time of arrival is plotted in Fig. 6(b) for a counting period of 580 h and agrees well with the calculated $R(\Delta t)$.

ACKNOWLEDGMENTS

It is a pleasure to acknowledge many helpful conversations with R. Kaplan and Professor S. Barone.